Particle Accelerators, 1992, Vols. 37–38, pp. 205–213
Reprints available directly from the publisher
Photocopying permitted by license only

© 1992 Gordon and Breach Science Publishers, S.A.
Printed in the United Kingdom

ENVELOPE MODEL OF A HEAVY-ION RECIRCULATOR†

W. M. SHARP, J. J. BARNARD and S. S. YU

Lawrence Livermore National Laboratory, Livermore, California 94550.

(Received 3 December 1990)

A simple transport code has been developed to model the beam in a heavy-ion recirculating accelerator. The novel feature of the model is the treatment of the beam charge density as a Lagrangian fluid in the axial direction. In addition, the envelope and centroid equations include terms that account for the transverse self-force, image forces, and bend fields in the paraxial limit. The use of "compressible" beam slices makes the code suitable for designing the acceleration and compression schedules. The code has been used primarily to design the lattice of the LLNL recirculator, and preliminary transport results for that machine are presented here.

1 INTRODUCTION

A recirculating accelerator for a heavy-ion fusion reactor requires detailed design of the lattice and the beam-acceleration schedule. The amount of energy gained by the beam per turn must be matched to the increase in the bend-magnet field strength, and the time variation of the acceleration field should be chosen to approximately balance the beam axial space-charge force. In addition, the injection and extraction sections must be effectively invisible to the beam except during the first and last turns, and the constraint that the undepressed phase advance per lattice period be less than about 80° must be satisfied at all times.

A fast-running envelope code has been developed to carry out the detailed lattice design for the Lawrence Livermore National Laboratory (LLNL) recirculating heavy-ion accelerator.[1] The model combines an envelope description of the beam transverse dynamics with a fluid-like treatment of axial dynamics. Appropriate terms are included to account for the effects of image forces, beam emittance, and space charge in the limit of paraxial motion, and the beam is focused and accelerated by a user-specified lattice of time-varying quadrupoles, bending magnets, and accelerating modules. In this paper, we briefly present the equations used in the model and discuss the code numerics. The concluding section gives code results for a preliminary lattice design, including a method for the final beam extraction.

† This work was performed under the auspices of the US Department of Energy by Lawrence Livermore National Laboratory under W-7405-ENG-48.

2 MODEL

The set of envelope equations used here to model the beam transverse dynamics is similar to that formulated first by Kapchinskij and Vladimirskij[2] and later adapted by Lee, Close, and Smith.[3] The beam transverse distribution function is assumed to be uniform and elliptical in each phase-space plane, and in the absence of an axial magnetic field the coordinate-space ellipse may be taken to be unskewed. The formulation differs from the more-rigorous envelope model of Chernin[4] mainly in representing the beam space charge by a perveance term, rather than obtaining it iteratively. As in Ref. 3, the treatment is first-order in the ratio of the beam radii and centroid displacements to the beam-pipe radius. This approximation makes it appropriate to represent bend magnets and quadrupoles by idealized expressions and to neglect higher-order multipole fields. In the present version of the code, only single-function magnets are used, and axial fringe fields are neglected. Although the ion mass is multiplied where it appears by the Lorentz factor γ, derivatives of γ are small enough to be dropped from the ion-motion equations. Also, we assume a circular beam pipe of infinite conductivity and radius R.

With these assumptions, the coupled envelope equations for the coordinate-space radii may be written as follows:

$$\frac{d^2a}{ds^2} + \frac{1}{\beta}\frac{d\beta}{ds}\frac{da}{ds} = \pm\frac{B'}{[B\rho]}a + \frac{\varepsilon_x^2}{a^3} + \frac{2K}{a+b} + \frac{fK}{R^2}a - \frac{a}{\rho^2} \tag{1a}$$

$$\frac{d^2b}{ds^2} + \frac{1}{\beta}\frac{d\beta}{ds}\frac{db}{ds} = \mp\frac{B'}{[B\rho]}b + \frac{\varepsilon_y^2}{b^3} + \frac{2K}{a+b} - \frac{fK}{R^2}b. \tag{1b}$$

Here, the notation of Ref. 3 is used without modification. The coordinate s is distance around the axis of the lattice, and x and y are respectively the spatial coordinates in and perpendicular to the plane of the lattice, with a and b being the beam coordinate-space radii in the x and y directions. The quadrupole-field transverse gradient is denoted by B', with the sign being determined by the magnet orientation. The "magnetic rigidity" in the quadrupole-focusing terms is given in SI units by

$$[B\rho] = \beta\gamma Mc/qe, \tag{2}$$

where M and q are the ion mass and charge state, β is the axial velocity scaled by the speed of light c, and γMc^2 is the total energy of beam ions. The perveance K in the space-charge and image-force terms is defined as

$$K = \frac{1}{4\pi\varepsilon_0}\frac{2qeI_b}{(\beta\gamma)^3Mc^3}, \tag{3}$$

where I_b is the beam current in amperes, and ε_0 is the free-space permittivity. The beam transverse temperature is accounted for in Eq. (1) by the terms proportional to the unnormalized emittances ε_x and ε_y, which are calculated in the present version of the code by assuming that the normalized-emittance components $\beta\gamma\varepsilon_x$ and $\beta\gamma\varepsilon_y$ are constant. The image-force terms in Eq. (1) were derived in Ref. 3 by assuming

that the centroid of the elliptical beam is displaced a distance $X \ll R$ from the axis of a straight beam pipe. With this assumption, the form of the coefficient f is

$$f(a, b, X) = \frac{a^2 - b^2}{4R^2} + \frac{X^2}{R^2}\left[1 + \frac{3}{2}\left(\frac{a^2 - b^2}{R^2}\right) + \frac{3}{8}\left(\frac{a^2 - b^2}{R^2}\right)^2\right]. \tag{4}$$

The presumption of a straight beam pipe substantially simplifies the algebra and is appropriate when the bend radius ρ is much larger than R. The two terms in Eq. (1) that differ from the envelope equation in Ref. 3 are $-a/\rho^2$ in the a equation, accounting for curvature of the beam-pipe axis with a local bend radius of ρ, and the $d\beta/ds$ terms, which arise from changing variables from t to s. As we discuss below, an approximate expression for $d\beta/ds$ is obtained directly from one of the equations for longitudinal motion.

As in Ref. 3, an equation for the lattice-plane centroid location X is obtained from a distribution average of the single-particle motion equations. The resulting equation may be written in the form

$$\frac{d^2X}{ds^2} + \frac{1}{\beta}\frac{d\beta}{ds}\frac{dX}{ds} = \pm\frac{B'}{[B\rho]}X + \left(\frac{1}{\rho} - \frac{B_y}{[B\rho]}\right) + \frac{gK}{R^2}X - \frac{X}{\rho^2}, \tag{5}$$

where the image-force coefficient g is given in the straight-pipe paraxial limit by

$$g(a, b, X) = 1 + \frac{a^2 - b^2}{4R^2} + \frac{X^2}{R^2}\left[1 + \frac{3}{4}\left(\frac{a^2 - b^2}{R^2}\right) + \frac{1}{8}\left(\frac{a^2 - b^2}{R^2}\right)^2\right]. \tag{6}$$

The term $-X/\rho^2$ in Eq. (5) again accounts for the lattice curvature, and we have chosen to use B_y explicitly in the momentum-difference term so that a bend field may be applied for extraction in a straight section of the lattice. The corresponding equation for the centroid y position is not included in the present code version.

The effects of the beam axial space charge are crucial to the operation of a heavy-ion recirculator both because the beam current affects the phase-advance depression and because the beam must be finally compressed to a small fraction of its initial length. To model axial dynamics, we treat slices of the beam as Lagrangian fluid elements characterized by an axial velocity βc and the time τ that the slice arrives at an axial location s. This approach implicitly assumes that the beam has a negligible longitudinal temperature and that the slices remain approximately collinear. If the slice boundaries are presumed to remain perpendicular to the beam-pipe axis, then the equation for τ is found from orbit kinematics to be

$$\frac{d\tau}{ds} = \frac{1}{\beta c}\left(1 + \frac{X}{\rho}\right), \tag{7}$$

where we have again assumed paraxial motion. An approximate β equation is obtained by retaining only the electrostatic force in the single-particle motion equations and averaging the axial component over the beam elliptical cross-section:

$$\frac{d\beta}{ds} = \frac{qe}{\beta Mc^2}\left(1 + \frac{X}{\rho}\right)(E_{\text{ext}} + E_{sc}). \tag{8}$$

Here, the average external electric field E_{ext} is approximated only by the voltage across accelerating modules divided by the gap length. The axial electric field induced by the change in bend-magnet field strength is neglected here because the field has a peak strength that is less than 0.1% of the average accelerating gradient and furthermore has a null on axis. The space-charge field is approximated by

$$E_{sc} \approx \frac{1}{4\pi\varepsilon_0}\left[\ln\left(\frac{2R^2}{a^2+b^2}\right)+\frac{1}{2}\right]\left[\frac{\partial}{\partial\tau}\left(\frac{\lambda}{\beta c}\right)+\frac{\lambda}{\beta}\frac{d\beta}{ds}\right], \tag{9}$$

where the line-charge density λ for a slice containing charge ΔQ is estimated by

$$\lambda = \frac{\Delta Q}{\beta c \Delta\tau}. \tag{10}$$

In deriving the space-charge field, the radial electrostatic field is assumed to vary over a much shorter scale length than E_{sc}, and the continuity equation is used to convert derivatives with respect to s into τ derivatives. When Eq. (9) is substituted into the β equation Eq. (8), the resulting equation is trivially rearranged to give an equation for $d\beta/ds$ in terms of E_{ext} and the time derivative of λ/β.

Equations (1)–(10) are recast in the code as a set of eight first-order equations and are integrated by a conventional fourth-order Runga–Kutta method. A constant step size in s is used in the present version, and the results are found to be insensitive to the choice of step size so long as there are 15 or more integration steps per lattice element. Since the envelope equations of Eq. (1) are quite complicated and may include quadrupoles of any length, commonly used expressions[5] for the averaged matched values of a and b are not, in general, useful for initializing the equations in equilibrium. Instead, we integrate the equations for a slice near the beam midpoint over the first full lattice period and adjust the initial values of the beam radii and their derivatives until they match the corresponding final values.

An important aspect of the code is the lattice specification. The user may specify an arbitrary number of distinct lattice elements, specifying appropriate properties such as length, aperture, strength, and bend angle. At present, the element types allowed in the code are drifts, accelerating gaps, sector bend magnets, and quadrupoles, but solenoids and higher-order multipoles may be easily added. Each lattice element is given a name by the user, and lattice sections may be defined by listing names of previously defined elements and subsections along with a repetition factor. The final such grouping of subsections is treated as the complete lattice, and the specification is checked to determine whether the lattice is a closed loop.

To facilitate code use, the code has a lattice "self-design" option. The main assumption used to modify the lattice parameters is that energy is gained linearly in distance s around the ring. With this assumption, the time-averaged voltage across accelerating gaps and the bend-field strengths and time derivatives may be set. Also, some compensation for longitudinal space charge is possible by imposing an appropriate time variation on the accelerating voltage. In this code, this voltage is allowed by vary up to quadratically with time, and the voltage-correction terms are

calculated from a four-term Legendre-series representation of the initial beam space charge.

3 RESULTS

Design work with the envelope code has focused on modeling the final ring of the four-ring LLNL ion recirculator. A tentative set of parameters for this ring is given in Table 1. The lattice for this ring consists of alternating 3.3 T focusing and defocusing superconducting quadrupoles with a half-lattice period L of 3 m and an occupancy $\eta \equiv L_{\text{quad}}/L = 0.2$. Between each pair of quadrupoles is a 1.2 m sector bend magnet flanked by a pair of accelerating gaps. The entire ring consists of 360 identical lattice periods and is 2160 m long. Although the bend-magnet drive voltage is planned to be a rising portion of a sine wave, the bend field B_y is assumed in the present simulations to increase linearly with time t and to be the same in all the bend magnets. This linear increase is the simplest to use because it corresponds to a constant energy gain per unit length. We use two accelerating gaps per quadrupole because this arrangement allows a better approximation to a linear energy gain than a one-gap configuration. A complete lattice design should also have straight sections on each side of the ring for beam injection and extraction, but we have chosen here to model these sections separately.

3.1 *Acceleration*

If a constant accelerating voltage is used, a beam pulse with the nominal parameters is found to lengthen by a factor of about three during the first pass around the lattice. The final line-charge density for this case is shown by the solid curve in Figure 1a, with the dashed line indicating the initial density profile. For an initial density

TABLE 1

Nominal Parameters for the High-Energy Ring of the LLNL Ion Recirculator

Beam parameters		
ion charge state	q	1
ion mass	M	200 amu
peak beam current	I_b	180 A
beam duration	τ_b	0.547 μs
initial energy	$(\gamma_0 - 1)Mc^2$	1 GeV
initial norm. emittance	$\gamma\beta\varepsilon_x$, $\gamma\beta\varepsilon_y$	10^{-5} m-rad
initial radius in x	a_0	4.8 cm
ininitial radius in y	b_0	2.6 cm
Lattice parameters		
length	$s_{\max}$	2160 m
half-period	L	3 m
pipe radius	R	6.7 cm
avg. energy gain	$Mc^2 d\gamma/ds$	83.3 kV/m

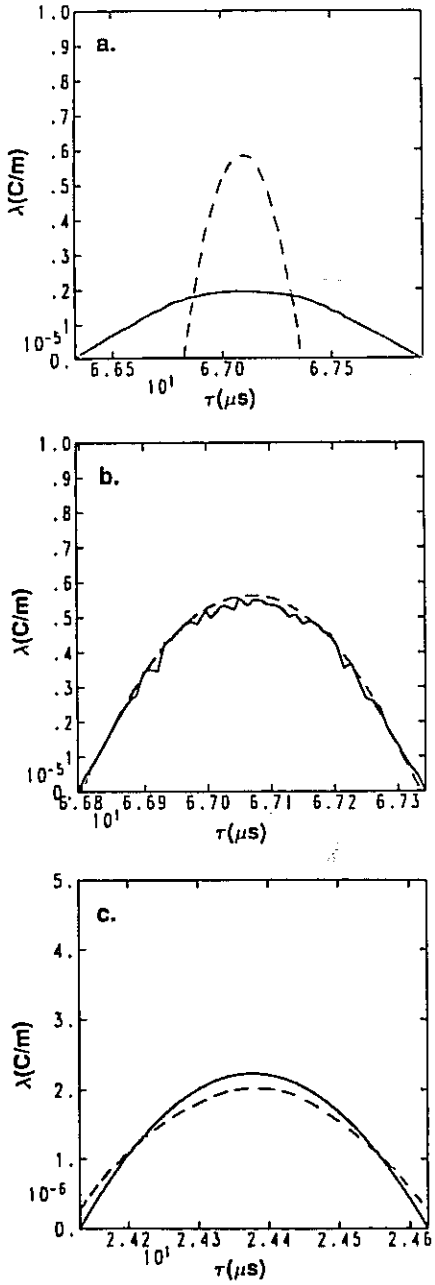

FIGURE 1 The beam line-charge density λ after one pass around the high-energy recirculator lattice with different initial conditions and accelerating schedules: (a) 1-GeV initial energy with a constant gap voltage; (b) 1-Gev initial energy with a linearly increasing gap voltage to balance space charge; (c) 9.82-GeV initial energy with the same linear voltage rise. The initial line-charge density is plotted as a dashed line in each case.

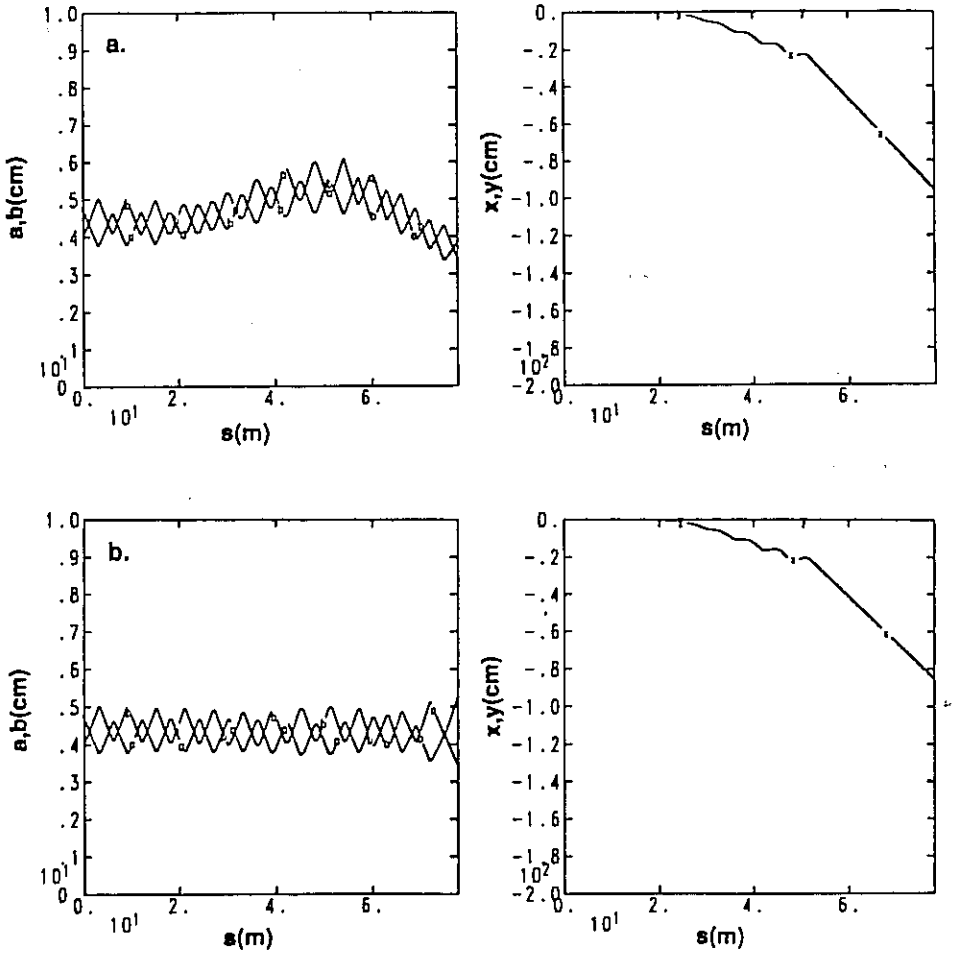

FIGURE 2 Envelope oscillations for a 10-GeV beam slice traversing two different extraction lattices: (a) a simple lattice with a single step in radius and constant $\eta B'$ throughout; (b) a lattice with a two-step radius change and quadrupole strength chosen to give a constant average a and b.

that varies parabolically with τ, the space charge force may be approximately cancelled by a suitable linear increase of the accelerating voltage with t. For a beam duration τ_b and a gap length L_{gap}, the appropriate time-varying part of E_{ext} is

$$\Delta E_{\text{ext}} \approx \frac{1}{4\pi\varepsilon_0}\left[\ln\left(\frac{2R^2}{\bar{a}^2+\bar{b}^2}\right)+\frac{1}{2}\right]\frac{4}{\tau_b}\frac{L}{L_{\text{gap}}}\frac{I_b}{\beta^2c^2}\left(1-\frac{2t}{\tau_b}\right), \tag{11}$$

where $\bar{a}$ and $\bar{b}$ are the matched beam radii averaged over a lattice period. If β in Eq. (11) is chosen to be the value appropriate for a 1 GeV beam, we find that the length of an initially parabolic beam is effectively unchanged at the end of the first pass through the lattice, as shown by the density plot of Figure 1b. A small

change in the beam profile is seen because $\bar{a}$, $\bar{b}$, and β do not remain uniform as the beam is accelerated.

Although pulse-forming lines can tailor the accelerating voltage to balance the space charge in the beam, even for beams with non-parabolic profiles, it is difficult to change the voltage time-dependence on successive passes. Since the beam velocity nearly triples in the final recirculator ring, the voltage rise chosen for the first pass would be too rapid for the last pass by about a factor of nine and would obviously compress the pulse. To see the extent of this compression, we ran a case using the same ΔE_{ext} and τ_b as in the first pass but with a beam energy and initial bend field appropriate for the last pass. The final calculated line-charge density, shown in Figure 1c, is found to be only about 10% shorter than the initial density profile, and the pulse remains nearly parabolic. The reason for this insensitivity is that the excessive external force is balanced by the larger space-charge force as the pulse compresses.

3.2 *Extraction*

Extraction from the final recirculator ring is complicated by the high magnetic rigidity of a 10-GeV heavy-ion beam. The method planned for the LLNL recirculator is to bend the beam away from the axis over several periods of a large-radius quadrupole lattice. A preliminary design uses eleven 1.2-m bend magnets, each with a strength of 0.34 T. The relatively weak field strength allows the magnets to be turned on between successive beam passes, and the odd number guarantees that the last bend be followed by a defocusing magnet. The first simulation attempt used six periods of quadrupoles with a 35 cm radius and occupancy η of 0.4. The strength was chosen to give constant $\eta B'$ because analytic estimates of $\bar{a}$ and $\bar{b}$ based on the "thin-lens" approximation[5] predict that this choice should give the same beam radii in the large quadrupoles as in the nominal ones. While this lattice allowed quite effective extraction, as seen in the X plot of Figure 2a, the radii of beam traversing the large quadrupoles with the bend field off increased by about 20%, as the plots of the variables a and b show, leaving the beam substantially mismatched.

To correct this effect of sudden changes in occupancy, we have worked out a more gradual extraction lattice. The quadrupole radii increase in two steps rather than one and in each section the quadrupole strength is determined iteratively to give the same $\bar{a}$ and $\bar{b}$ as the nominal lattice. Also, following the last large quadrupole the occupancy of the nominal-radius quadrupoles is decreased in two steps, with the strength again adjusted to keep the radii the same. This modified lattice gives the same extraction as the first, as the X plot of Figure 2b shows, but the a and b plots with the bend field off show that the beam remains much better matched.

REFERENCES

1. S. S. Yu, J. J. Barnard, G. J. Caporaso, A. Friedman, D. W. Hewitt, H. Kirbie, M. A. Newton, V. K. Neil, A. C. Paul, L. L. Reginato, W. M. Sharp, R. O. Bangerter, C. G. Fong, D. L. Judd and T. F. Godlove, "Constraints on recirculating induction-driver designs," these *Proceedings*.
2. I. M. Kapchinskij and V. V. Vladirmirskij, in *Proceedings of the International Conference High Energy Accelerators* (CERN, Geneva, 1959), p. 274.

3. E. P. Lee, E. Close, and L. Smith, "Space charge effects in a bending magnet system," in *Proceedings of the 1987 IEEE Particle Accelerator Conference*, edited by E. R. Lindstrom and L. S. Taylor (IEEE, New Jersey, 1987), p. 1126.
4. D. Chernin, *Part. Accel.* **24**, 29 (1988).
5. E. P. Lee, T. J. Fessenden, and L. J. Laslett, "Transportable Charge in a Periodic Alternating Gradient System," Lawrence Berkeley Laboratory report No. LBL-19560 (1985).